INVESTIGATIONS OF A CYCLONE DUST COLLECTOR

by

WILLIAM WOODROW DODGE

B. S., Oklahoma Agricultural and Mechanical College, 1941

M. S., Kansas State College
of Agriculture and Applied Science, 1949

A THESIS

submitted in partial fulfillment of the

requirements for the degree

MASTER OF SCIENCE

Department of Applied Mechanics

KANSAS STATE COLLEGE
OF AGRICULTURE AND APPLIED SCIENCE

1951

TABLE OF CONTENTS

INTRODUCTION

The important variables in dust collection seem to be obscure or not too well known. The work reported in the literature appears to have little grounds on which to base a correlation between workers. Much data have been reported on operational variables such as inlet velocity, temperature, inlet to outlet area ratio, while sufficient data to establish geometrical similarity are mostly lacking. Generally the dust collectors used differ so greatly in proportions that there is little or no geometrical similarity.

It is the purpose of this research to study certain of these variables which affect the efficiency of collection in the cyclone dust collector. The collectors may vary in regard to inlet height and width, outlet area, cylindrical section diameter and height and cone length. The density, viscosity and inlet velocity of the gas may have an appreciable effect on the efficiency of collection. The size, density, shape, surface and particle size distribution of the dust are variables to be considered. In this work the variation of physical dimensions such as cone length, inlet shape, inlet to outlet ratio, height of cylindrical section and distance to which the outlet tube extends down into the collector were studied.

Inlet velocity and pressure drop are two operational variables which were included in this study. Temperature of the fluid and other operational variables were not included for study. A dust was selected upon its suitability with regards to fineness, avail-

ability, and physical and chemical inertness for use as a standard of comparison.

LITERATURE SURVEY

Pressure Drop Theory

Lissman (1) assumes the law of conservation of angular momentum, and that the expansion of the gas is isothermal, in deriving a formula for draft loss across the cyclone dust collector. An attempt is made to show that, for similar cyclones, the draft loss is independent of the dimensions of the collector, and is a function of tangential velocity and density of the gas only.

$$P_1 - P = 0.288 \frac{W_1}{g} V_1^2$$

where

$P_1 - P$ = draft loss--inches Water gage,

W_1 = density of gas #/ft.^{3}

V_1 = tangential velocity in outer vortex.

Shepherd & Lapple (2) obtain the empirical relationship for friction loss in a cyclone with an inlet deflecting vane

$$F_{cv} = 7.5 \frac{bh}{e^2} \; .$$

They (3) obtained, in like manner, a formula for a cyclone without an inlet deflecting vane.

$$F_{cv} = 16 \frac{bh}{e^2}$$

F_{cv} = Friction loss across cyclone

e = exit tube diameter

h = inlet height

b = inlet width

Briggs (4) states that for a given rate of gas flow the decrease in pressure drop, with the addition of dust, is proportional to the square root of the dust concentration. This amounts to as much as 16 per cent less pressure drop. He gives the following empirical equation:

$$\frac{Po - P}{Po} = 0.13 \ C \quad .$$

where

Po = Pressure drop without dust.

P = Pressure drop with dust.

C = dust concentration $\frac{\text{grains}}{\text{ft.}^3}$

Velocity Distribution

A general equation introduced by Shepherd & Lapple (2) will be used to represent the tangential velocity at any point in the outer vortex of the cyclone dust collector, of the form

$$V = V_o \left(\frac{r_o}{r}\right)^n$$

where

V_o = tangential velocity at radius r_o (reference velocity)

V = tangential velocity at radius r

n = a constant exponent

This equation will facilitate the comparison of the various tangential velocity distributions reported in the literature. Lissman assumed an idealized fluid for which $n = 1$.
Seillan (5) and Mill Mutual (6) state that the air in the outer vortex moves with constant angular velocity or $n = -1$.

Prokat (7) gives an experimentally determined value of $n = 0.7$. Shepherd & Lapple (2) determined the value of $n = 0.5$ from experimental observations.

Rosin, Rammler and Intelmann (8) assumed the value of $n = 0$, giving a constant tangential velocity at every point in the outer vortex.

Collection Efficiency

Lissman (1), with the above mentioned assumptions, calculated the values of acceleration in the outer vortex, and stated that the collection efficiency decreased as the diameter of the cyclone increased. Anderson (9), Whiton (10), and Parent (11) show, experimentally, that this is the case. Their collectors range collectively from 2 to 126 inches in diameter.

Briggs (4) shows that collection efficiency increases very slightly as the dust concentration increases. He also shows that the collection efficiency increases very slightly as the pressure drop increases. Parent (11) states that the collection efficiencies of the cyclones used were not affected by the dust loadings in the range encountered.

Parent (11) also reports that if the density of the gas is quadrupled by an increase pressure then the velocity would need to be one-half as much to get the same pressure drop, temperature being the same. This would indicate a lower collection efficiency.

Whiton (10) and Parent (11) present data to indicate that collection efficiency decreases as the temperature of the gas increases. The range of temperature covered in these experiments was from 80° to 1000° F.

Whiton (10), Anderson (9) and Parent (11) show that as the inlet velocity is increased, the collection efficiency increases.

Rosin, Rammler and Intelmann (8) make certain simplifying assumptions, and starting with Stokes law for spheres settling in a fluid derive an equation for the minimum size sphere collectable in a cyclone dust collector.

$$D_{p(min)} = \sqrt{\frac{9M\ (r_2 - r_1)}{\pi N V_t(\rho_s - \rho_{fl}}}$$

where

$D_{p(min)}$ = theoretical minimum sized particle collectible

M = fluid viscosity

$r_2 - r_1$ = width of cylindrical annular space

$_s$ = density of particles

$_{fl}$ = density of fluid

V_t = tangential velocity

N = theoretical number of turns the gas takes in passing through the annular space.

Shepherd and Lapple (12) feel that the $(r_2 - r_1)$ term should be replaced by the radius of the exit tube. They also state that a fractional separation x should be obtained on particles of size Dx, smaller than Dmin when

Dx = Dmin $x(2-x)^n$. They give no derivation of this formula.

Van Tongeren (13) states that there is a double eddy current in the cyclone dust collector similar to that encountered in the fluid flowing around an elbow. Shepherd and Lapple (2), in a very extensive search, state that they cannot find this phenomenon.

MATERIALS AND METHODS

The experimental setup is shown in Plates 1 and 2. The air enters the system through the ASME long radius nozzle shown at the left of Plate I. A Pitot tube of the Prandtl type is located in the center of the duct after the nozzle for the determination of velocity and flow. The inlet through which the dust is introduced into the air stream by the motor driven dust feeder is located about 6" down the pipe from the nozzle. Following this the air and dust travel through about eight feet of duct before entering the cyclone dust collector. A glass jar is at the bottom of the collector to hold the dust during collection. The U tube manometer, seen on the table beside the collector in Plate I, is used to measure pressure drop across the collector. It is connected to taps at the inlet and outlet of the collector. The outlet tube is located at the top of the collector. This tube takes the air and uncollected dust on to the inlet of the fan shown in Plate II. Just ahead of the fan is a slide valve for shutting off the flow between samples without shutting off the motor. The air and uncollected dust are then discharged to the atmosphere through the vertical duct connected to the outlet of the fan. At the bottom of Plate II can be seen the Reeves Variable speed drive. Plate III shows the experimental set up for taking tangential velocity measurements. The pitot tube used to measure the tangential velocities in the collector was of the Prandtl type with an outside diameter of 1/16".

The nozzle in Plate I was made of plaster and cement with a throat diameter of six inches. This type of inlet was used to

EXPLANATION OF PLATE I

Front view of equipment.

PLATE I

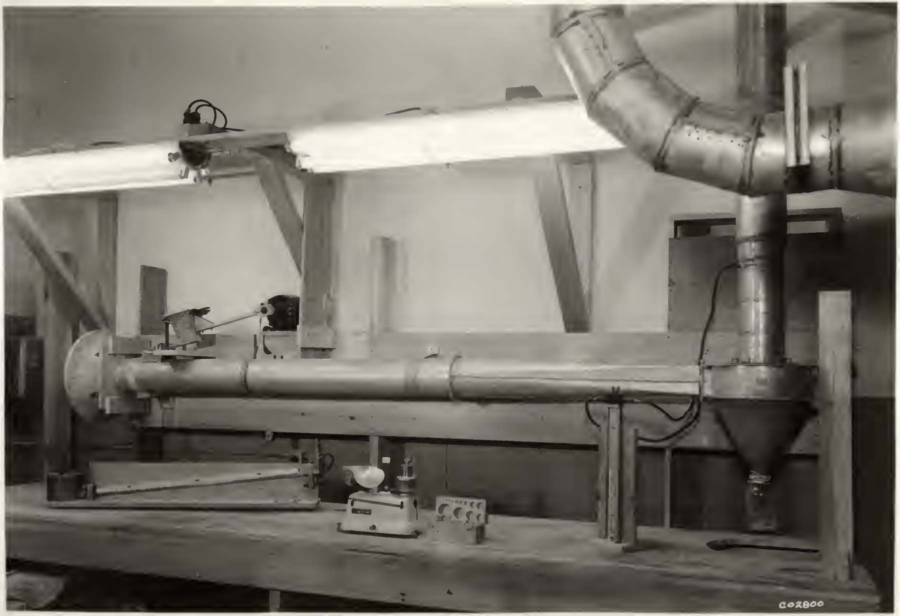

EXPLANATION OF PLATE II

Motor, speed changer and fan.

PLATE II

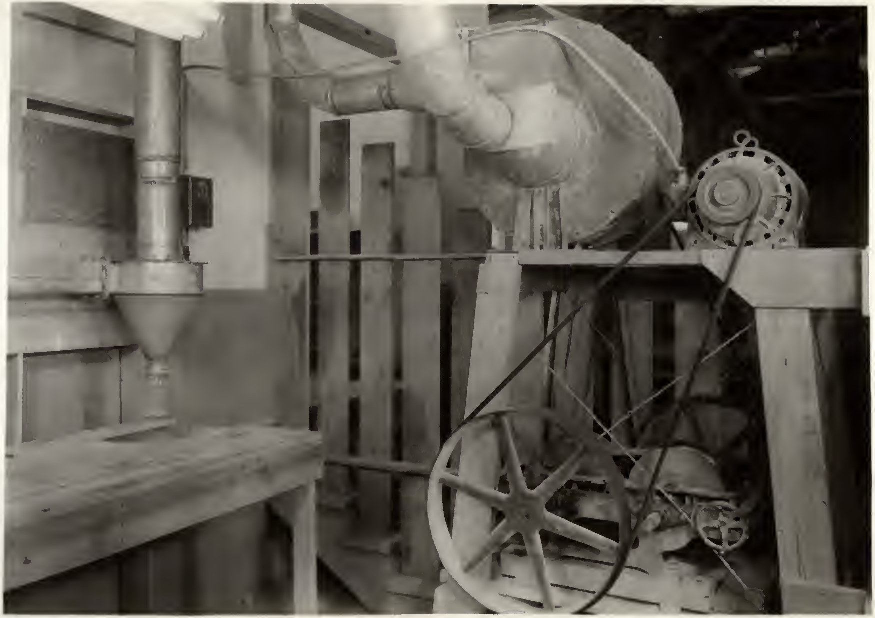

give a flat velocity profile at the entrance for simplicity of velocity and flow calculations. The velocity profile was checked experimentally and found to be flat as indicated by Prandtl and Tietjens (16).

Immediately after the inlet the pitot tube was placed at the center of the duct, to measure the velocity head of the entering air, from which the velocity and flow were calculated. Connected to the pitot static tube is an inclined draft gage which may be seen immediately below on the table. This manometer contained oil of 0.9135 specific gravity but was calibrated to read in inches of water.

The dust feeder was constructed with an airtight hopper to contain the 500 grams of dust used in each run. This feeder was actuated by an electric motor with a variable throw eccentric. The throw and angle of inclination of the feeder outlet tube were adjusted to give the desired rate of feed. The speed of the motor was fixed.

After the addition of the dust to the air stream, the dust laden air was passed through about eight feet of 6" duct and a transition section before entering the dust collector. This was for the purpose of allowing the dust and air to become thoroughly mixed.

The dust collectors used in this research were made in sections to facilitate varying the physical dimensions so that the effect of these dimensions upon collection efficiency and pressure drop could be studied. The diameter of the cylindrical section was held constant at 12 inches. The cross sectional area of the

EXPLANATION OF PLATE III

Collector, pitot tube and manometer as used for tangential velocity determinations.

PLATE III

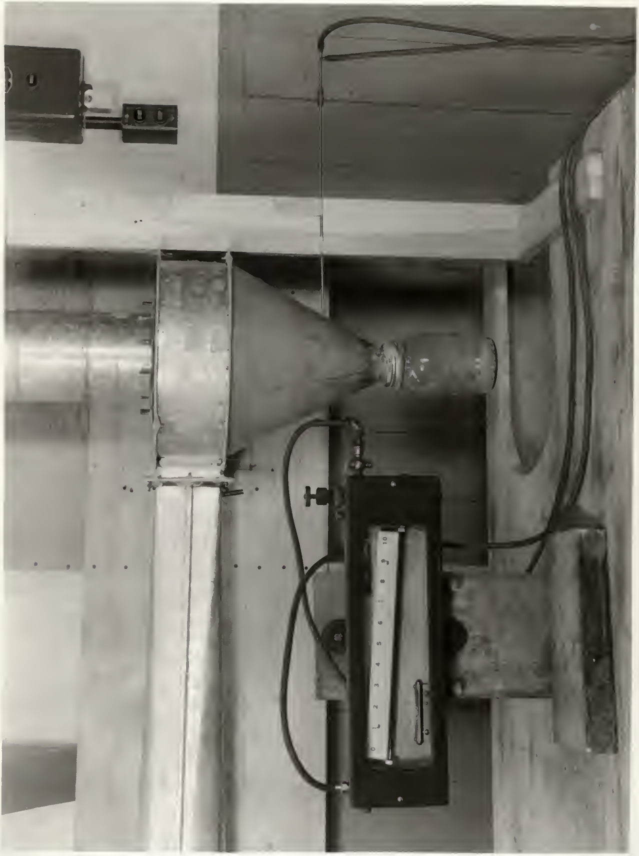

EXPLANATION OF PLATE IV

Cylindrical sections with inlet and transition.

PLATE IV

EXPLANATION OF PLATE V

Dimension drawing of equipment in Plate IV.

PLATE V

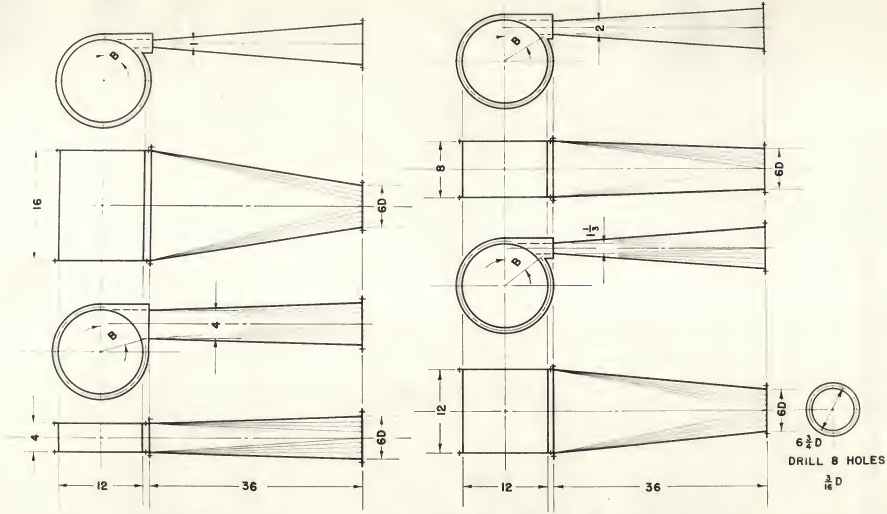

NOTE 1 - ALL FLANGES $\frac{3}{4}$ WIDE

ALL DIMENSIONS IN INCHES

NOTE 2 - BOLT CIRCLES $12\frac{3}{4}$ IN DIAM. WITH $\frac{3}{16}$D BOLTS SPACED AT 15° INTERVALS, EXCEPT IN ANGLE B.

inlet was held constant at 16 square inches. Entry of the air into the collector was tangential, Plates IV and V.

The dust collectors will be referred to by code; e.g., 16 - 4 - 1 - D. The 16 indicates that the cylindrical section 16" high was used. The 4 represents the cone length in diameters while the 1 is the ratio of outlet to inlet area. The D indicates that the outlet tube is in the down position.

The conical sections are pictured in Plate VI with a dimension drawing appearing in Plate VII. These cones were made in lengths of from 1 to 4 diameters. It is logical to assume that if the cone length is increased sufficiently that eventually there will be a decrease in efficiency, the same would be true when shortening the cone. It was hoped that the most efficient cone length obtainable would fall between 1 diameter and 4 diameters. This was found not to be the case.

The outlet tubes and cyclone covers were connected by a sliding joint shown in Plates VIII and IX. There were three outlets made having cross sectional areas of 0.67, 1.0, and 1.5 times the inlet area. They were made to allow the tube to extend a maximum distance of 17 inches into the dust collector.

The fan in Plate II was a 30 inch Buffalo Planning Mill Exhauster. It was driven by a 5 hp motor through a Reeves Variable speed drive size 0. The range of speed variation for the fan was from 600 to 2600 R.P.M. This gave a range of pressure drop up to 12 inches of water and a collector inlet velocity range of from 2500 to 4400 feet per minute.

The dust, used in these experiments, was finely ground Ottawa

PLATE VI

EXPLANATION OF PLATE VII

Dimension drawing of cone sections.

EXPLANATION OF PLATE VI

Cone sections.

PLATE VII

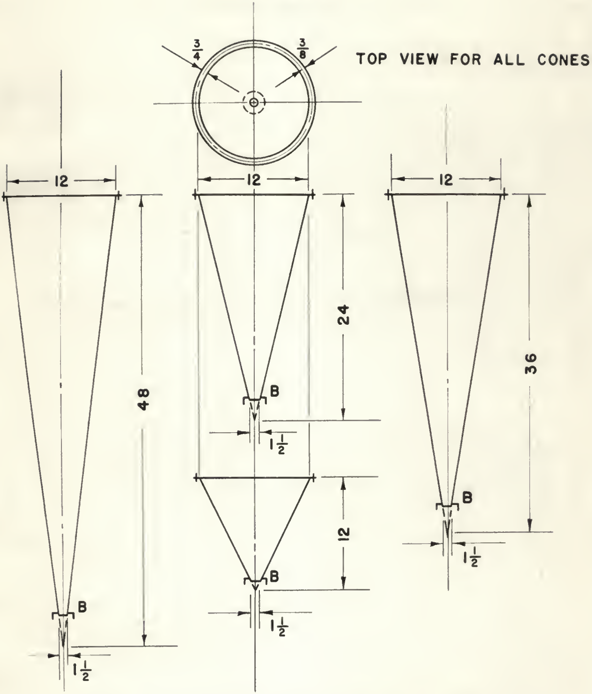

NOTE – B – CONNECTION FOR DUST CONTAINER

ALL DIMENSIONS IN INCHES

EXPLANATION OF PLATE VIII

Outlet tubes with sliding collector covers.

PLATE VIII

EXPLANATION OF PLATE IX

Dimension drawing of outlet tube and covers.

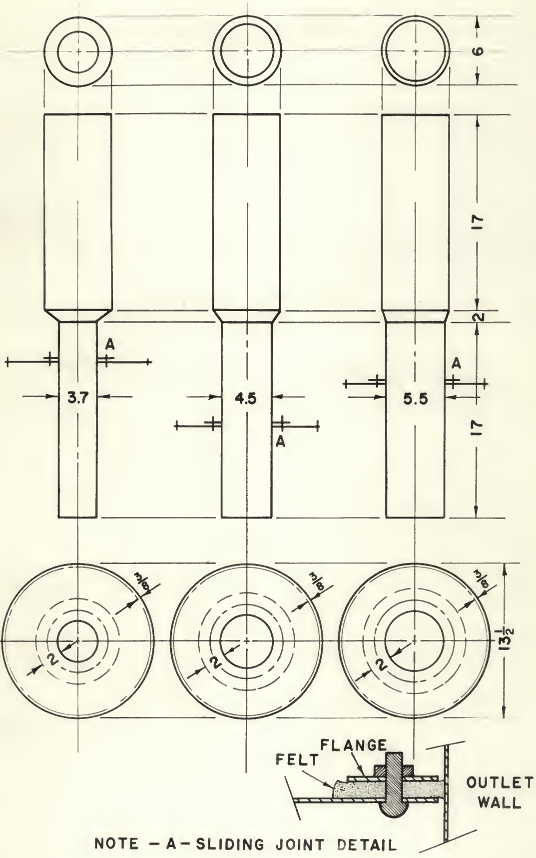

NOTE — A — SLIDING JOINT DETAIL

ALL DIMENSIONS IN INCHES

Silica Sand. This dust was tested for fineness by the permeability method, (ASTM method No. C204-46T) (14), and found to have a specific surface of 3440 square centimeters per gram. A Bureau of Standards sample of Portland Cement, having a specific surface of 3300 square centimeters per gram, was used as a standard of comparison. The results of a sieve analysis run according to the method of Wichser et al. (15) are shown in Table 1.

Table 1. Sieve analysis of dust.

	Percent
over 150 mesh	trace
over 200 mesh	4.0%
over 270 mesh	13.5%
over 325 mesh	21.5%
over 400 mesh	29.5%
thru 400 mesh	70.5%

This particular dust was chosen because of its chemical and physical inertness, and its availability for use as a standard of comparison.

A series of ten identical collection runs with all variables held constant was made to determine the variability of the tests. A standard deviation of 0.48 per cent was calculated from the data with the use of the following formula; Snedecor (17)

$$S = \sqrt{\frac{\underline{X}^2 - \frac{(\underline{X})^2}{N}}{N}}$$

where

S = standard deviation

$\underline{X}$ = individual test result

N = number of replicates.

With this as a basis it was considered that a 500 gram sample would give sufficient accuracy for this work. It was also determined that the 500 gram sample was fed into the stream in 3.66 minutes which gives a rate of feed of 136.5 grams per minute. At an average inlet velocity of 3500 feet per minute the quantity of flow is 389 cubic feet per minute. Dividing 389 by 136.5 gives a loading of 2.85 grams of dust per cubic foot of air or 44.0 grains per cubic foot.

EXPERIMENTAL

The experimental data taken in this research appear in Table 2 (Appendix) master table, from which the data for each of the graphs have been taken.

Effect of Inlet Velocity on Collection Efficiency

Figure 1 is a graph of collection efficiency vs inlet velocity for the 4 basic dust collectors. The 4 basic collectors are defined as 16 - 4 - 1.5 - D, 12 - 3 - 1.5 - D, 8 - 2 - 1.5 - D and 4 - 1 - 1.5 - D because they span the range of efficiencies expected. In all 4 cases the efficiency increases as the velocity increases. The curve for 8 - 2 - 1.5 - D levels off at about 92 per cent while the other three curves continue to increase over the ranges of velocity investigated.

From a consideration of vortex motion it is reasonable to assume that the tangential velocity throughout the collector will increase as the inlet velocity is increased. A consideration of the velocities and accelerations discloses two forces acting on a particle within the collector. The most important of these is the centrifugal force $\frac{w}{g} \frac{V_t^2}{r}$. This is the force that brings about separation of the dust from the gas. The other force is the force of drag which may be considered as consisting of turbulent mixing and true drag.

The exact determination of these forces and their action on various size particles is beyond the scope of this work.

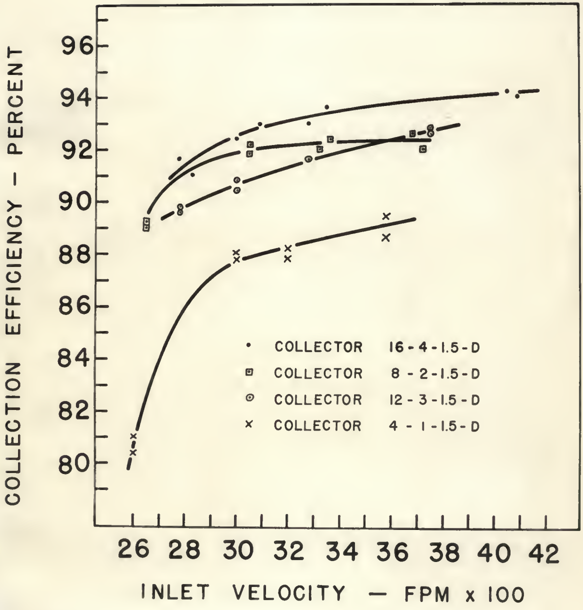

Fig. 1. The effect of inlet velocity on collection efficiency.

Outlet Area versus Collection Efficiency

Figure 2 shows the effect of inlet velocity on collection efficiency for three different outlet areas. In general it can be seen that collection efficiency increases as the outlet area is decreased except at the lower inlet velocities. Although a greater efficiency is obtained at the higher velocities this must be compensated for by greatly increased power requirements as the pressure drop would indicate. The curves for the 0.67 and the 1.0 ratio outlet do not appear to be statistically very different. They are much higher than that representing the 1.5 ratio outlet. This increase in efficiency might be due to the fact that the particles are forced to go farther radially inward before reaching the outlet tube to escape. In being forced closer to the center line the particles will have a greater centrifugal force and they should have a better chance of being collected. It is also possible in the case of the 1.5 ratio outlet that, after the particle has reached a point where the radial forces are in equilibrium, the drag force upward is greater than the force of gravity downward. If the outlet tube is large enough to include much of the outer vortex much dust might be lost that could have been collected.

Velocity and Pressure Distribution

Figure 3 is a map of tangential velocities at the various positions throughout collector 4 - 1 - 1.5 - D as shown. The data for Figure 3 appear in Table 3. This is a map of the air

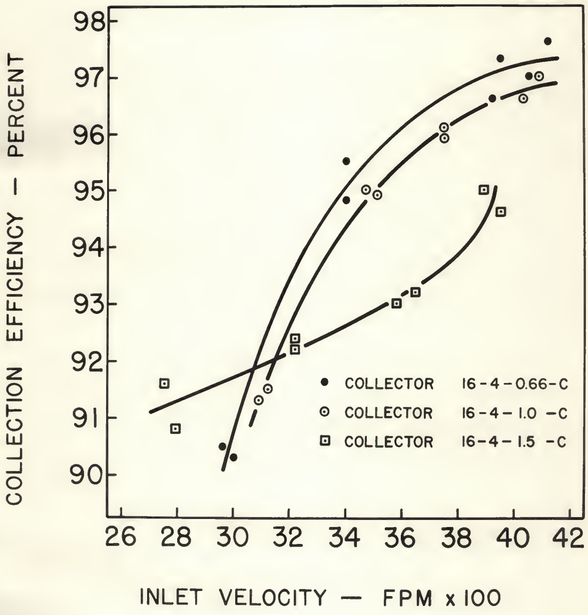

Fig. 2. The effect of outlet area on collection efficiency for various inlet velocities.

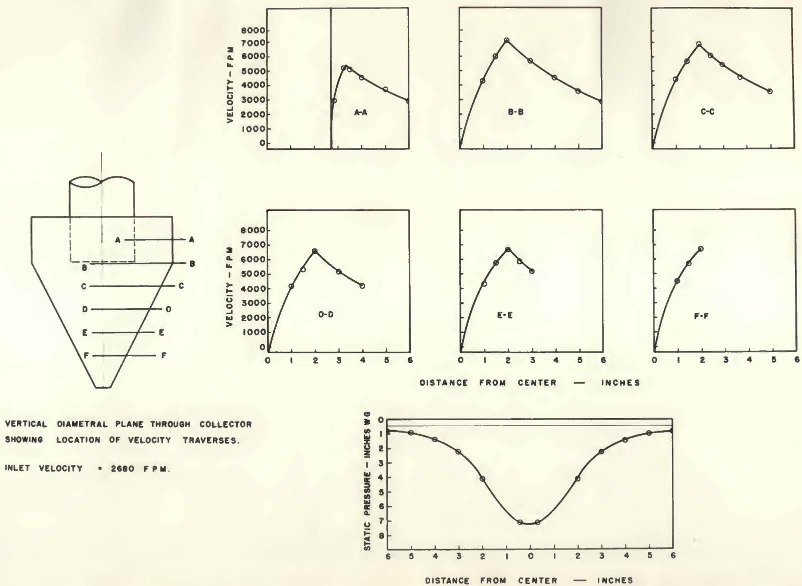

Fig. 3. Tangential velocity and static pressure distribution in collector 4 - 1 - 1.5 - D.

Table 3. Velocity map data.

Distance from center, inches	Tangential vel. F.P.M.	Distance from center, inches	Tangential Vel. F.P.M.
	4 - 1 - 1.5 - D		
Section AA		Section BB	
6.00	2920	6.00	2950
5.00	3750	5.00	3620
4.00	4585	4.00	4660
3.75	5130	3.00	5740
3.50	5220	2.00	7100
2.90	3000	1.50	6000
		1.00	4350
Section CC		Section DD	
5.00	3630	4.00	4220
3.75	4370	3.00	5270
3.00	5180	2.00	6600
2.50	6100	1.50	5310
2.00	6950	1.00	4100
1.50	5640		
1.00	4310		
Section EE		Section FF	
3.00	5050	2.00	6500
2.50	5800	1.50	5540
2.00	6550	1.00	4350
1.50	5700		
1.00	4260		

Static pressures compared with atmospheric pressure

Distance from center, inches	Static pressure inches, W. G.
6.0	-0.78
5.0	-0.91
4.0	-1.37
3.0	-2.19
2.0	-4.11
0.3	-7.03
Static pressure at inlet	-0.46
Static pressure at outlet	-4.75

velocities without dust as dust would clog the pitot tube, making accurate readings impossible. As is shown, there were six velocity traverses along diameters of the cyclone. It was found that the velocity profiles were symmetrical with respect to the center line in all cases. For that reason only half of the velocity profiles are shown. Traverse A - A runs from the wall of the outlet tube to the outside wall of the collector. The other five traverses run from the center line to the wall of the collector. When the wall is reached the curves stop at the last velocity reading. It is obvious that the pitot tube used was incapable of detecting the boundary layer. No attempt was made to represent the boundary layer as equipment for taking measurements in the boundary layer was not available. The velocities in Traverse A - A near the outlet tube wall might appear to resemble a boundary layer but it is likely that this resemblance is due to the distortion of the inner vertex by the outlet tube wall. Rouse (18) developed the Rankine combined vortex for an ideal fluid. In the case studied friction appears to have caused a deviation from theory. The most noticeable deviation from theory is in the inner vortex where the velocities do not follow a straight line relationship. It can be seen in Figure 3 that the velocities from $r = o$ to $r = 2$ curve slightly with the slope decreasing gradually. This is very likely due to the effects of friction and turbulence. The mathematics required to develop this are far too complicated for this paper. If the notation of Shepherd & Lapple (2) is used and n is determined from the end velocities in the outer vortex a value of $n = 0.8$ is obtained. For a frictionless fluid the value of n would be 1.

It can easily be observed that the isovels are vertical right circular cylinders. With this in mind a hypothesis of collection can be constructed. The primary forces, centrifugal and drag, acting on a particle in the collector are each proportional to the square of the velocity. It can be shown from Figure 3 and flow net theory that the tangential velocity is much greater than the radial velocity. From this it can be inferred that the centrifugal force is greater than the drag force for a given particle at the pt. of maximum tangential velocity. Referring to Figure 3 section B - B, if a particle is assumed to be in the velocity field at a point near the outer wall, then it is conceivable that the drag force could be greater than the centrifugal force. This being the case the particle would migrate down and toward the center of the collector. As it did, however, the centrifugal force would increase as the square of the velocity or as much as eight times, while the Drag force would not increase greatly. Considering the particle collectible somewhere between $r = 6$ and $r = 2$ inches in this instance the drag and centrifugal forces would become equal and the particle would stop its radial motion. At this point it would then depend on whether the vertical velocity were up or down. If the vertical velocity were down the particle would migrate down and out in a spiral of increasing radius due to a decrease of the drag force. In the case of the particle coming to radial equilibrium at a point where the vertical velocity was upward, then the particle would be lost out the outlet. This would be likely only near the outlet tube which might be the reason why a greater efficiency is obtained with the outlet tube extending

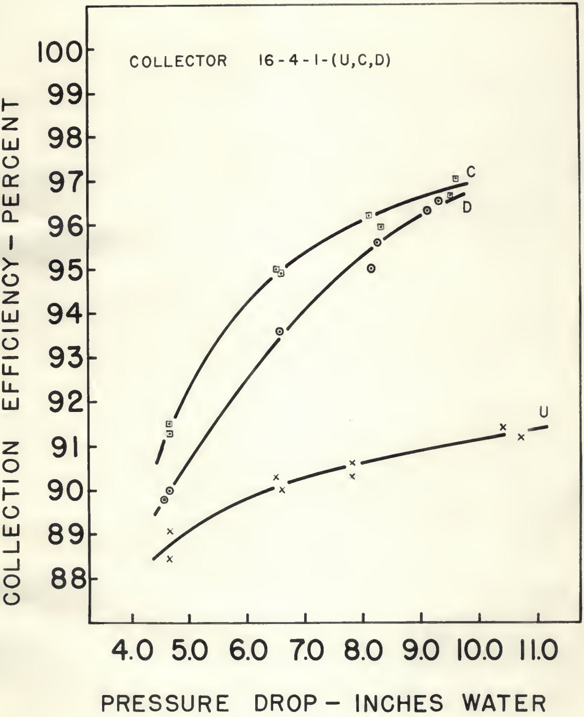

Fig. 4. The effect of outlet tube position on collection efficiency.

Table 4. Power consumption.

Test no.	Inlet vel. with dust FPM	ΔP with dust feet water	C.F.M.	Ft. #/min.	Eff %
		16 - 4 - 1.5 - D			
127	2780	0.233	308	4,495	91.6
128	2830	0.225	314	4,410	91.0
129	3090	0.283	343	6,050	93.0
130	3000	0.283	333	5,880	92.4
131	3280	0.342	364	7,770	93.0
132	3350	0.342	372	7,945	93.6
133	4050	0.400	450	11,215	94.2
134	4090	0.400	459	11,455	94.0
		12 - 3 - 1.5 - D			
215	2780	0.150	308	2,880	89.8
216	2780	0.150	308	2,880	89.6
217	3000	0.217	333	4,510	90.4
218	3000	0.225	333	4,685	90.8
219	3280	0.308	364	7,000	91.6
220	3360	0.308	373	7,145	91.8
221	3750	0.375	417	9,765	92.6
222	3750	0.383	417	9,865	92.8
		8 - 2 - 1.5 - D			
271	2650	0.283	294	5,185	89.0
272	2650	0.283	294	5,185	89.2
273	3050	0.358	339	7,545	91.8
274	3050	0.358	339	7,545	92.2
275	3320	0.433	369	9,950	92.0
276	3360	0.433	373	10,225	92.4
277	3680	0.550	409	14,020	92.6
278	3720	0.558	413	14,380	92.0
		4 - 1 - 1.5 - D			
82	2600	0.291	389	5,260	81.0
81	2600	0.283	289	5,115	80.4
80	3000	0.383	333	7,965	88.0
79	3000	0.367	333	7,620	87.8
78	3240	0.425	360	9,540	88.2
77	3200	0.417	356	9,250	87.8
76	3580	0.516	397	12,755	89.4
75	3580	0.525	397	13,000	88.6

into the collector. This will be shown in a later figure.

Collection Efficiency versus Pressure Drop

Figure 4 shows collection efficiency versus pressure drop across the collector for three different positions of the outlet tube. The center position (C) is the most efficient but is only slightly better than the down position (D) especially for the higher pressure drops. The up-position (U) is considerably less efficient than the other two positions. The low efficiency of the up position may have resulted from a portion of the air taking a shortcut from the inlet to the outlet. This would give less opportunity for the dust to be collected. A greater noise was observed during runs when the tube was in the up position which may be an indication of the air taking the short-cut.

Collection Efficiency versus Power Consumption

Figure 5 is a plot of collection efficiency against power consumption in ft. lb/min. It appears in 3 cases that the efficiency increases very rapidly up to a power consumption of about 8000 ft. lb/min. after which it increases very little in all four cases. As might be expected the 4 - 1 - 1.5 - D is the least efficient of the four basic collectors. This might be due in part to the short time of retention of the air and dust in the collector. It could also be due partially to the shape of the inlet. In the 16 - 4 - 1.5 - D collector the inlet is long and narrow which causes all of the dust to enter the collector near the outside wall. With the 4 - 1 - 1.5 - D, 3/4 of the dust

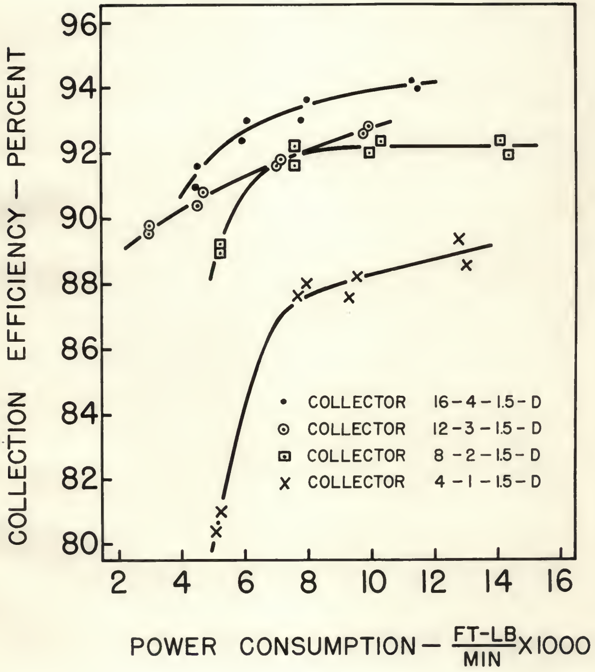

Fig. 5. Power consumption vs. collection efficiency.

enters the collector farther from the wall than in the 16 - 4 - 1.5 - D collector. The values for power consumption are not to be taken as an accurate estimate of the power consumption. The rotation of the gas in the outlet tube increases the static pressure at the wall due to the centrifugal force. An accurate value for the static pressure, against which the fan is working, can be obtained from the following equation.

$$P = \frac{\int_A P d_A}{A} \qquad (1)$$

The pressure losses or gains in the collector may be separate into three parts; first, that due to friction, second that due to the outlet area being different from the inlet area, third the loss caused by conversion of pressure energy into kinetic energy of rotation in the outlet.

Pressure Drop versus Inlet Velocity

Figure 6 is a plot of pressure drop across the collector against inlet velocity. Each curve taken separately is not far from being linear. The curves for 16 - 4 - 1.5 - D and 12 - 3 - 1.5 - D would indicate that these collectors required less pressure drop to produce a given inlet velocity. This might be due to a smoother entry when the stream is relatively flat.

If all 4 curves are considered in the average, they give the effect of a linear increase of pressure drop when the inlet velocity is increased.

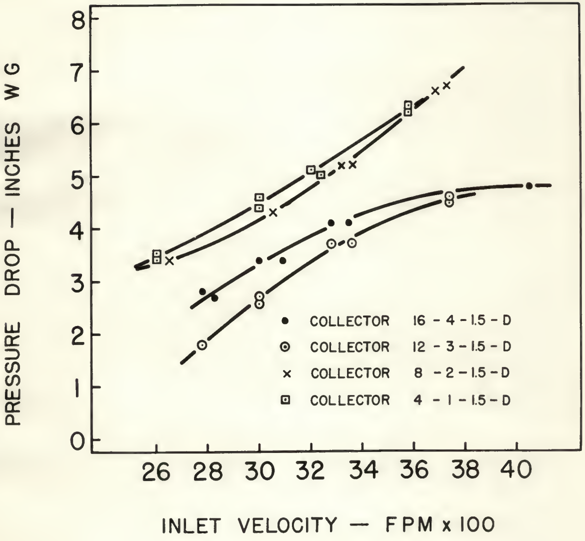

Fig. 6. The effect of inlet velocity on pressure drop.

Effect of Dust upon Pressure Drop

Green (20) presents evidence to support the view that when particles are suspended in a fluid the apparent viscosity of the suspension is greater than that of the fluid. Figure 7 and Table 5 show the effect of adding dust on the relationship between pressure drop and inlet velocity. The upper curve is a plot of the pressure drop and inlet velocity for the collector without dust. Dust was introduced into the air stream after which the velocity was adjusted to the original valve and the pressure drop was read. The lower curve is a plot of these values. Calculations show that the introduction of the dust caused a decrease in pressure drop of from 12 to 24 percent. When dust is added the decrease in pressure drop appears proportional to the pressure drop.

If one considers a boundary layer containing dust it seems reasonable to assume that the presence of dust particles rolling and bounding along with the flow will increase the fluid turbulence in the boundary layer. This would be greater if the diameter of the particles was larger than the thickness of the boundary layer due to a greater velocity of the particle.

Prandtl and Tietjens (19), show that as the boundary layer becomes turbulent the drag force on a sphere actually decreases with increasing velocity. The possibility suggests itself that the increase in turbulence caused by the particle causes the wall friction force to decrease in a similar manner. The use of Reynolds number to describe the flow in this case seems to be

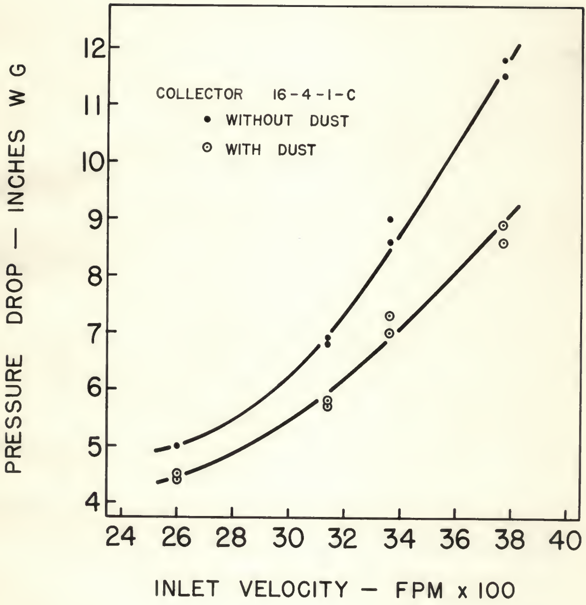

Fig. 7. The effect of dust on the pressure drop across a cyclone dust collector.

Table 5. Effect of dust addition.

Test no.	Inlet vel. w/o dust FPM	Inlet vel. w. dust FPM	P w/o dust in WG	P w. dust in WG	Eff %
		16 - 4 - 1 - C			
322	2600	2600	5.0	4.4	85.0
321	2600	2550	5.0	4.5	84.8
320	3140	3140	6.8	5.8	88.2
319	3140	3180	6.9	5.7	88.6
35	3360	3360	9.0	7.3	90.4
34	3360	3360	8.6	7.0	90.0
33	3785	3785	11.8	8.9	92.8
32	3780	3780	11.5	8.6	93.0

out of the question because of the difficulty in picking a characteristic dimension and velocity.

Effect of Cone Length and Inlet Shape upon Collection Efficiency

The effect of cone length on collection efficiency for all four cylindrical sections is shown in Figure 8. When the 1 diameter cone was used it was found that the efficiencies were not statistically different for the cylindrical sections. As the cone length was increased, the 4 inch cylindrical section was found to be most efficient with the 12 inch section being least efficient. The curves for 4 - _ - 1.5 - D and 8 - _ - 1.5 - D level off at 3 diameters. The curves for 16 - _ - 1.5 - D and 12 - _ - 1.5 - D have not reached a maximum efficiency at 4 diameters.

An attempt was made to maintain inlet velocity constant for all the tests in this graph. An inspection of Table (6) reveals that the velocity varied, between tests, from 3680 to 3240 F.P.M.

At first, the data from the graph might appear contradictory to some of the data in preceding figures. In Figure 1 collector 16 - 4 - 1.5 - D was most efficient in all cases. Upon checking it was found the second highest set of valves for 16 - 4 - 1.5 - D in Figure 1 is identical with the highest set of valves in Figure 8 for 16 - - 1.5 - D. The same is correspondingly true for the other three curves in Figure 1. In Figure 2 collector 16 - 4 - 1.5 - C has an efficiency, at a comparable velocity of 3610 ft/min, of 93.1 per cent. As the outlet area is decreased, Figure 2, the efficiency goes up much higher than anything in Figure 8, e.g., 97.6 per cent.

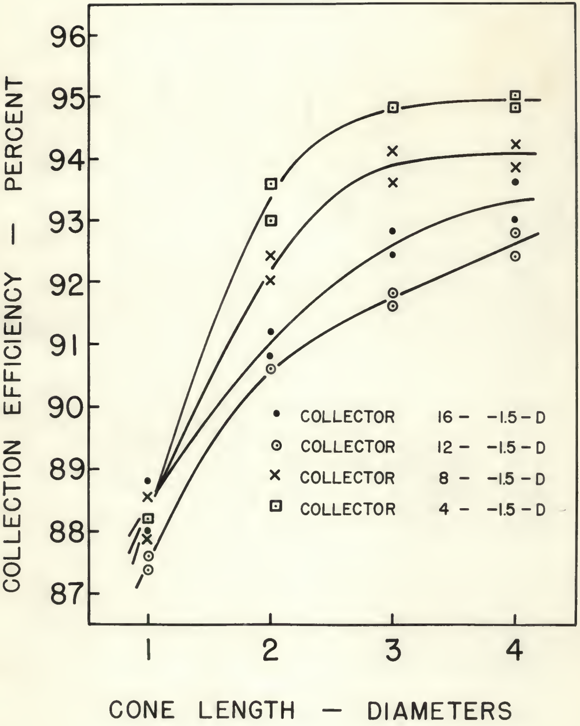

Fig. 8. The effect of cone length on collection efficiency for four different shape inlets.

Table 6. Cone length data.

Test no.	In. vel. w/o dust FPM	In. vel. w. dust FPM	Δ P w/o dust in WG	Δ P w. dust in WG	Eff %
			16 - - 1.5 - D		
131	2970	3280	4.2	4.1	93.0
132	2970	3350	4.1	4.1	93.6
155	2970	3240	4.4	4.0	92.4
156	2970	3320	4.3	4.0	92.8
161	3010	3640	4.8	4.6	90.8
162	3010	3610	4.7	4.5	91.2
171	3040	3680	4.8	4.7	88.0
172	3040	3640	4.8	4.7	88.8
			12 - - 1.5 - D		
227	3040	3360	3.6	3.5	92.4
228	3050	3360	3.7	3.6	92.8
219	3050	3280	3.8	3.7	91.6
220	3050	3360	3.8	3.7	91.8
235	3040	3360	3.7	3.7	90.6
236	3040	3400	3.7	3.7	90.6
243	3050	3360	4.0	4.0	87.4
244	3050	3330	3.9	4.0	87.6
			8 - - 1.5 - D		
299	3090	3360	5.3	5.2	94.2
300	3040	3360	5.4	5.3	93.8
307	3040	3400	5.0	4.8	93.6
308	3040	3440	5.1	4.8	94.1
275	3010	3320	5.3	5.2	92.0
276	3010	3360	5.3	5.2	92.4
315	3040	3360	4.5	4.5	88.2
316	3040	3440	4.5	4.5	88.2
			4 - - 1.5 - D		
123	3010	3400	4.6	4.6	94.8
124	3010	3330	4.6	4.6	95.0
115	2970	3360	5.0	4.8	94.8
116	2970	3360	5.0	4.9	94.8
107	2970	3260	4.9	4.8	93.0
108	2970	3320	5.2	5.1	93.6
77	2970	3200	5.3	5.0	87.8
78	2970	3240	5.3	5.1	88.2

SUMMARY

The collection efficiency of a cyclone dust collector increased as the inlet velocity was increased. As the outlet area was increased the collection efficiency decreased. The position of the outlet tube which gave the best efficiency was where the outlet tube extended into the collector half the height of the inlet. The collection efficiency was found to increase as the length of cone increased. The square inlet was found to give better collection efficiency than the rectangular shapes. The tangential velocities and static pressures were found to correspond closely to those in a Rankine combined vortex. From these results an hypothesis of the path a particle takes in passing through the collector was advanced.

ACKNOWLEDGMENTS

The author wishes to thank Professors Shellenberger and Farrell of the Department of Milling Industry and Professors Holander and Duncan of the Department of Mechanical Engineering for the loan of equipment used in this research. This work would not have been possible without the enthusiastic support of Professor Scholer, Head of the Department of Applied Mechanics, K. S. C. The author is indebted to Professor Gerald Pickett of the Department of Applied Mechanics for his very able assistance in this research and in preparing the manuscript. Also special thanks are due to Mrs. Stewart and Miss Otto for help in typing and preparing the manuscript.

BIBLIOGRAPHY

(1) Lissman, M. A.
Mechanical methods of dust collection. Chem. and Met. Engr. 37:630-634, Oct. 1930.

(2) Shepherd, C. B. and C. E. Lapple.
Flow pattern and pressure drop in cyclone dust collectors. Ind. and Eng. Chem. 31:972-984, August, 1939.

(3) Shepherd, C. B. and C. E. Lapple.
Flow pattern and pressure drop in cyclone dust collectors. Ind. and Eng. Chem. 32:1146-1248, September, 1940.

(4) Briggs, L. W.
Effect of dust concentration on cyclone performance. A.I.Ch.E. Trans. 42:511-526, 1946.

(5) Seillan.
Note sur les Depoussiereur Centrifuges, Chaleur et Industrie. 233-38, 289-293, May, June, 1929.

(6) Engineering Service Department, Mill Mutual Fire Prevention Bureau. Cyclone collectors Bulletin No. DC-350, February, 1947.

(7) Prokat, F.
Glasers Ann. 107:43-45, 47-54, 1930.

(8) Rosin, P., E. Rammler and W. Intelmann.
Z. Vern. Deut. Ing. 76:443-447, 1932.

(9) Anderson, E.
Effect of tube diameter in cyclonic dust collectors. Chem., and Met. Engr. 40:525-526, October, 1933.

(10) Whiton, L. C., Jr.
Performance characteristics of cyclone dust collectors. Chem, and Met. Engr. 39:150-152, March, 1932.

(11) Parent, J. D.
Efficiency of small cyclones (aerotec) as a function of loading, temperature and pressure drop. A.I.Ch.E. Trans. 42:989-999, 1946.

(12) Lapple, C. E. and C. B. Shepherd.
Calculation of particle trajectories, Ind. and Eng. Chem. 32:605-617., May, 1940.

(13) Van Tongeren, Herman.
A modern dust collector. Mech. Engr. 57:753-759. December, 1935.

(14) ASTM C204-46T.
Fineness of portland cement by air permeability apparatus. ASTM Philadelphia, 1950.

(15) Wichser, F. W., J. A. Shellenberger & R. O. Pence.
Relationship of the physical properties of wheat flour to granulation. Cereal Chem. 24:381-393. November, 1947.

(16) Prandtl, L. and O. G. Tietjens.
Applied hydro and aero mechanics. New York: McGraw-Hill, 1934.

(17) Snedecor, G. W.
Statistical methods. 4th ed. Ames, Iowa: Iowa State College Press, 1946.

(18) Rouse, H.
Fluid mechanics for hydraulic engineers. New York: McGraw-Hill, 1938.

(19) Prandtl, L. and O. G. Tietjens.
Applied hydro and aero mechanics. New York: McGraw-Hill, 1934.

(20) Green, Henry.
Industrial rheology and rheological structures. New York: John Wiley, 1949.

APPENDIX

Table 2. Master table.

Test no.	Inlet vel. w/o dust FPM	Inlet vel. w. dust FPM	Δ P w/o dust in WG	Δ P w. dust in WG	Eff %
		16 - 4 - 1 - D			
A		3200	6.5	6.3	94.0
B		3230	6.4	6.2	93.8
C		3185	6.5	6.2	93.0
D		3210	6.5	6.3	94.0
E		3200	6.4	6.2	93.8
F		3240	6.3	6.1	93.0
G		3210	6.5	6.3	92.6
H		3160	6.4	6.3	93.4
I		3190	6.3	6.1	93.8
J		3210	6.5	6.2	94.0
		16 - 4 - 0.67 - D			
43	2550	2960	5.1	5.0	87.2
42	2550	2960	5.0	4.8	87.2
41	2970	3430	7.0	6.8	89.0
40	2970	3430	7.1	6.9	88.5
39	3360	3770	9.2	9.1	89.6
38	3360	3750	9.4	9.1	89.4
37	3550	3920	10.7	10.4	90.0
36	3550	3920	11.0	10.8	88.2
		16 - 4 - 0.67 - C			
44	2510	2960	5.0	4.8	90.5
45	2550	3000	4.9	4.8	90.3
46	2970	3400	6.8	6.7	95.5
47	2930	3400	6.7	6.6	94.8
48	3330	3950	8.9	8.6	97.3
49	3300	3920	8.8	8.7	96.6
50	3580	4050	10.2	10.0	97.0
51	3580	4120	10.3	9.9	97.6
		16 - 4 - 0.67 - U			
327	2500	2770	5.2	5.0	82.6
328	2500	2770	5.0	4.8	82.4
329	2790	3040	7.1	6.9	83.8
330	2800	3060	7.1	6.8	84.0
331	3100	3660	8.7	8.5	86.8
332	3140	3660	8.6	8.3	87.0
333	3600	3960	10.0	9.7	87.6
334	3580	3940	10.1	9.8	87.2

Table 2. (cont.)

Test no.	Inlet vel. w/o dust FPM	Inlet vel. w. dust FPM	△P w/o dust in WG	△P w. dust in WG	Eff %
		16 - 4 - 1 - D			
14	2550	2960	4.9	4.6	90.0
13	2600	3000	5.0	4.6	89.8
12	3010	2400	7.0	6.6	93.6
11	3050	3430	7.1	6.6	93.6
10	3300	3910	8.7	8.1	95.0
9	3320	3950	8.7	8.2	95.6
8	3540	4400	10.5	9.1	96.3
7	3530	4400	10.5	9.3	96.5
		16 - 4 - 1 - C			
15	2600	3090	5.0	4.7	91.3
16	2610	3120	5.0	4.7	91.5
17	3050	3510	7.0	6.6	94.9
18	3050	3470	6.9	6.5	95.0
19	3400	3750	8.8	8.3	95.9
20	3400	3750	8.6	8.1	96.2
21	3640	4090	10.0	9.6	97.0
22	3610	4030	9.9	9.5	96.6
		16 - 4 - 1 - U			
31	2550	2920	4.9	4.7	88.4
30	2550	2940	5.0	4.7	89.1
28	2960	3320	6.8	6.6	90.0
27	2960	3360	6.9	6.5	90.3
26	3240	3580	8.2	7.8	90.7
25	3200	3580	8.1	7.8	90.3
24	3710	4240	11.1	10.4	91.4
23	3710	4220	11.2	10.7	91.3
		16 - 4 - 1.5 - D			
127	2440	2780	2.8	2.8	91.6
128	2440	2830	2.8	2.7	91.0
129	2660	3090	3.4	3.4	93.0
130	2660	3000	3.4	3.4	92.4
131	2970	3280	4.2	4.1	93.0
132	2970	3350	4.1	4.1	93.6
133	3280	4050	5.1	4.8	94.2
134	3280	4090	5.1	4.8	94.0

Table 2. (cont.)

Test no.	Inlet vel. w/o dust FPM	Inlet vel. w. dust FPM	Δ P w/o dust in WG	Δ P w. dust in WG	Eff %
		16 - 4 - 1.5 - C			
142	2440	2790	2.7	2.7	90.8
141	2440	2750	2.7	2.6	91.6
140	2750	3220	3.5	3.4	92.2
139	2750	3220	3.4	3.3	92.4
138	2970	3580	4.1	3.9	93.0
137	3010	3650	4.1	3.8	93.2
136	3330	3890	5.1	5.0	95.0
135	3330	3950	5.2	4.9	94.6
		16 - 4 - 1.5 - U			
143	2500	2930	2.6	2.5	88.2
144	2450	2970	2.6	2.4	89.0
145	2750	3360	3.3	2.9	88.6
146	2750	3290	3.3	3.0	89.0
147	2970	3590	3.9	3.5	88.0
148	2970	3650	3.9	3.5	88.4
149	3330	4010	5.1	4.5	86.6
150	3330	4010	5.0	4.6	86.8
		16 - 3 - 1.5 - D			
151	2440	2750	2.8	2.6	89.6
152	2440	2790	2.8	2.6	89.0
153	2700	3050	3.5	3.4	91.4
154	2700	3010	3.5	3.3	91.8
155	2970	3240	4.4	4.0	92.4
156	2970	3320	4.3	4.0	92.8
157	3300	3690	5.3	4.9	93.2
158	3300	3650	5.2	5.9	93.0
		16 - 2 - 1.5 - D			
166	2440	2930	3.0	2.8	88.6
165	2440	2970	2.9	2.8	89.0
164	2700	3260	3.7	3.4	90.2
163	2740	3260	3.7	3.5	90.6
162	3010	3640	4.8	4.6	90.8
161	3010	3610	4.7	4.5	91.2
160	3360	4020	5.8	5.6	93.2
159	3360	4050	5.8	5.6	94.0

Table 2. (cont.)

Test no.	Inlet vel. w/o dust FPM	Inlet vel. w. dust FPM	Δ P w/o dust in WG	Δ P w. dust in WG	Eff %
			16 - 1 - 1.5 - D		
167	2400	2740	2.9	2.8	85.4
168	2400	2790	3.0	2.8	85.0
169	2740	3060	3.9	3.8	86.8
170	2740	3100	3.8	3.7	87.0
171	3040	3680	4.8	4.7	88.0
172	3040	3640	4.9	4.7	88.8
173	3400	3820	6.0	5.9	87.2
174	3360	3790	6.0	5.8	87.0
			12 - 3 - 1.0 - D		
191	2500	2700	3.6	3.4	91.4
192	2500	2700	3.5	3.3	91.8
193	2750	3260	4.5	4.1	92.2
194	2750	3180	4.6	4.1	92.6
195	3010	3440	5.8	5.5	93.0
196	3050	3470	5.8	5.4	93.2
197	3360	3890	7.2	6.9	94.2
198	3330	3850	7.3	6.9	94.0
			12 - 3 - 1.0 - C		
190	2440	2740	3.5	3.3	92.2
189	2440	2740	3.6	3.4	92.6
188	2700	3220	4.4	4.1	92.8
187	2700	3260	4.5	4.1	93.0
186	3010	3400	5.7	5.3	93.0
185	3010	3440	5.7	5.3	92.2
184	3320	3820	7.3	6.9	94.2
183	3360	3920	7.3	6.9	94.2
			12 - 3 - 1.0 - U		
175	2440	2740	3.7	3.5	89.0
176	2440	2740	3.7	3.5	88.6
177	2740	3100	4.7	4.5	88.6
178	2740	3100	4.7	4.5	88.2
179	3060	3400	6.0	5.8	89.4
180	3060	3400	5.9	5.7	90.0
181	3360	3920	7.4	7.1	86.0
182	3360	3890	7.4	7.1	85.6

Table 2. (cont.)

Test no.	Inlet vel. w/o dust FPM	Inlet vel. w. dust FPM	ΔP w/o dust in WG	ΔP w. dust in WG	Eff %
		12 - 3 - 1.5 - D			
215	2500	2780	1.8	1.8	89.8
216	2500	2780	1.8	1.8	89.6
217	2700	3000	2.9	2.7	90.4
218	2740	3000	2.8	2.6	90.8
219	3050	3280	3.8	3.7	91.6
220	3050	3360	3.8	3.7	91.8
221	3360	3750	4.8	4.6	92.6
222	3360	3750	4.8	4.5	92.8
		12 - 3 - 1.5 - C			
207	2500	2750	2.2	2.0	90.2
208	2500	2750	2.2	2.0	90.4
209	2750	3050	2.9	2.7	90.8
210	2750	3050	2.9	2.8	91.0
211	3010	3360	4.0	3.8	91.8
212	3010	3330	4.0	3.8	92.2
213	3360	3750	4.6	4.5	92.6
214	3360	3750	4.6	4.5	93.0
		12 - 3 - 1.5 - U			
199	2500	2750	2.0	1.9	80.8
200	2500	2790	2.0	1.9	80.4
201	2750	3010	2.7	2.7	82.2
202	2700	3010	2.7	2.6	82.0
203	3010	3290	3.6	3.5	83.4
204	3050	3330	3.6	3.4	83.2
205	3360	3750	4.1	3.9	81.8
206	3360	3720	4.0	3.9	82.0
		12 - 4 - 1.5 - D			
223	2500	2750	2.3	2.2	90.2
224	2500	2750	2.3	2.3	90.0
225	2750	3100	3.0	2.8	93.0
226	2750	3100	3.0	2.8	92.6
227	3040	3360	3.6	3.5	92.4
228	3050	3360	3.7	3.6	92.8
229	3330	3650	4.5	4.3	92.8
230	3330	3650	4.4	4.2	92.8

Table 2. (cont.)

Test no.	Inlet vel. w/o dust FPM	Inlet vel. w. dust FPM	ΔP w/o dust in WG	ΔP w. dust in WG	Eff %
		12 - 2 - 1.5 - D			
231	2500	2750	2.2	2.2	87.6
232	2500	2790	2.3	2.2	87.2
233	2700	3040	2.8	2.7	89.8
234	2700	3040	2.9	2.7	90.2
235	3040	3360	3.7	3.7	90.6
236	3040	3400	3.7	3.7	90.6
237	3400	3690	4.7	4.7	91.4
238	3360	3770	4.6	4.6	91.8
		12 - 1 - 1.5 - D			
239	2500	2750	2.5	2.7	84.2
240	2500	2790	2.6	2.7	84.2
241	2750	3100	3.2	3.4	86.8
242	2790	3140	3.2	3.4	86.2
243	3050	3360	4.0	4.0	87.4
244	3050	3330	3.9	4.0	87.6
245	3360	3690	4.7	4.8	88.6
246	3360	3650	4.7	4.9	88.4
		8 - 2 - 1.0 - D			
254	2500	2760	5.8	5.5	91.2
253	2500	2750	5.7	5.4	91.6
252	2750	3040	7.6	7.1	93.2
251	2750	2970	7.5	7.1	93.6
250	3040	3400	8.7	8.4	94.0
249	3040	3360	8.7	8.3	93.8
248	3330	3720	10.9	10.2	94.2
247	3260	3690	11.0	10.4	94.0
		8 - 2 - 1.0 - C			
262	2450	2790	6.0	5.9	93.0
261	2450	2740	6.1	5.9	93.6
260	2740	3050	7.9	7.7	93.4
259	2790	3050	8.0	7.8	93.8
258	3010	3330	9.6	9.3	94.8
257	3010	3360	9.7	9.3	94.6
256	3330	3720	11.1	10.6	95.6
255	3330	3720	11.2	10.6	95.4

Table 2. (cont.)

Test no.	Inlet vel. w/o dust FPM	Inlet vel. w. dust FPM	△ P w/o dust in WG	△ P w. dust in WG	Eff %
		8 - 2 - 1.0 - U			
263	2500	2840	6.4	6.2	87.2
264	2500	2840	6.5	6.3	86.6
265	2740	3050	8.1	7.9	87.2
266	2740	3050	8.0	7.9	87.6
267	3010	3360	9.2	9.2	87.0
268	3010	3400	9.3	9.2	86.6
269	3290	3750	11.1	11.0	84.9
270	3330	3790	11.1	11.0	85.0
		8 - 2 - 1.5 - D			
271	2500	2650	3.5	3.4	89.0
272	2500	2650	3.5	3.4	89.2
273	2650	3050	4.3	4.3	91.8
274	2650	3050	4.3	4.3	92.2
275	3010	3320	5.3	5.2	92.0
276	3010	3360	5.3	5.2	92.4
277	3360	3680	6.6	6.6	92.6
278	3360	3720	6.7	6.7	92.0
		8 - 2 - 1.5 - C			
279	2500	2740	2.9	2.9	90.0
280	2500	2740	3.0	3.0	90.2
281	2740	3010	4.4	4.3	93.2
282	2740	3010	4.4	4.3	92.4
283	3010	3330	5.1	5.0	92.2
284	3010	3360	5.1	5.0	92.8
285	3360	3690	6.4	6.3	93.0
286	3360	3690	6.4	6.3	92.6
		8 - 2 - 1.5 - U			
287	2500	2750	3.3	2.8	81.2
288	2500	2750	3.3	2.8	81.6
289	2750	3010	4.1	3.8	84.0
290	2750	3010	4.1	3.9	84.6
291	3010	3330	4.9	4.8	85.0
292	3010	3330	4.9	4.8	84.8
293	3360	3690	6.2	6.1	84.0
294	3360	3690	6.3	6.2	83.4

Table 2. (cont.)

Test no.	Inlet vel. w/o dust FPM	Inlet vel. w. dust FPM	Δ P w/o dust in WG	Δ P w. dust in WG	Eff %
		8 - 4 - 1.5 - D			
295	2550	2750	4.6	4.6	89.0
296	2550	2750	4.7	4.6	88.4
297	2750	3100	5.0	4.9	90.4
298	2750	3050	5.0	4.9	91.4
299	3040	3360	5.3	5.2	94.2
300	3040	3360	5.4	5.3	93.8
301	3360	3650	6.5	6.4	92.0
302	3360	3690	6.5	6.4	91.6
		8 - 3 - 1.5 - D			
303	2500	2750	2.9	2.9	91.0
304	2500	2710	3.0	2.9	91.0
305	2750	3100	3.8	3.7	92.6
306	2750	3100	3.6	3.6	92.2
307	3040	3400	5.0	4.8	93.6
308	3040	3440	5.1	4.8	94.1
309	3360	3720	6.4	6.2	95.2
310	3360	3720	6.5	6.2	94.8
		8 - 1 - 1.5 - D			
311	2500	2790	2.9	2.8	90.6
312	2500	2790	2.9	2.9	90.0
313	2750	3050	3.7	3.7	92.0
314	2750	3140	3.8	3.7	92.2
315	3040	3360	4.5	4.5	88.2
316	3040	3440	4.5	4.5	88.2
317	3400	3720	5.7	5.6	95.2
318	3360	3720	5.8	5.8	94.8
		4 - 1 - 1.0 - D			
58	2400	2740	6.1	5.1	82.8
57	2390	2700	6.2	5.9	83.0
56	2700	2960	7.4	7.1	87.4
55	2700	2920	7.4	7.1	86.2
54	2920	3280	9.1	8.6	87.4
53	2970	3360	9.6	9.2	87.8
52	3220	3540	10.7	10.2	88.0
51	3260	3570	10.8	10.1	87.8

Table 2. (cont.)

Test no.	Inlet vel. w/o dust FPM	Inlet vel. w. dust FPM	Δ P w/o dust in WG	Δ P w. dust in WG	Eff %
		4 - 1 - 1.0 - C			
66	2400	2650	6.1	5.8	85.6
65	2400	2700	6.1	5.9	84.8
64	2700	3000	7.7	7.3	87.8
63	2750	3120	8.2	7.8	87.8
62	2970	3360	9.2	8.9	90.0
61	2970	3400	9.7	9.0	89.4
60	3220	3680	10.6	10.4	90.2
59	3260	3570	10.0	10.3	90.6
		4 - 1 - 1.0 - U			
67	2440	2650	6.2	6.0	84.0
68	2440	2700	6.2	6.0	83.6
69	2700	3000	7.6	7.3	88.4
70	2700	3000	7.6	7.3	87.6
71	2970	3280	9.2	8.9	89.8
72	2920	3320	9.2	8.9	89.2
73	3220	3540	11.0	10.4	89.8
74	3220	3580	11.8	10.2	89.2
		4 - 1 - 1.5 - D			
82	2380	2600	3.7	3.5	81.0
81	2380	2600	3.7	3.4	80.4
80	2740	3000	4.8	4.6	88.0
79	2740	3000	4.7	4.4	87.8
78	2960	3240	5.3	5.1	88.2
77	2960	3200	5.3	5.0	87.8
76	3240	3580	6.6	6.2	89.4
75	3200	3580	6.7	6.3	88.6
		4 - 1 - 1.5 - C			
83	2390	2650	3.6	3.6	83.4
84	2390	2600	3.6	3.5	83.8
85	2750	3050	4.4	4.4	88.2
86	2750	3050	4.4	4.3	88.0
87	2970	3320	5.1	5.0	88.6
88	3010	3320	5.0	4.9	88.6
89	3220	3610	6.0	5.9	89.2
90	3260	3640	5.9	5.8	89.4

Table 2. (concl.)

Test no.	Inlet vel. w/o dust FPM	Inlet vel. w. dust FPM	ΔP w/o dust in WG	ΔP w. dust in WG	Eff %
		4 - 1 - 1.5 - U			
98	2500	2690	3.1	3.3	80.4
97	2500	2690	3.1	3.4	80.2
96	2700	2910	3.7	3.9	81.8
95	2750	2930	3.7	3.9	81.8
94	2970	3210	4.8	4.7	82.6
93	2970	3170	4.8	4.7	82.2
92	3260	3540	5.9	5.8	83.2
91	3260	3540	5.9	5.7	82.8
		4 - 4 - 1.5 - D			
119	2450	2790	3.1	3.1	93.0
120	2450	2750	3.1	3.1	92.4
121	2750	3100	3.8	3.9	94.2
122	2750	3100	3.8	3.8	94.6
123	3010	3400	4.6	4.6	94.8
124	3010	3330	4.6	4.6	95.0
125	3330	3720	5.6	5.6	95.2
126	3330	3650	5.7	5.7	94.6
		4 - 3 - 1.5 - D			
111	2440	2750	3.0	2.9	92.6
112	2440	2750	3.1	3.0	93.0
113	2700	3050	4.1	4.0	94.8
114	2700	3050	4.2	4.0	94.2
115	2970	3360	5.0	4.8	94.8
116	2970	3360	5.0	4.9	94.8
117	3260	3650	6.0	5.7	95.6
118	3260	3620	6.0	5.7	95.4
		4 - 2 - 1.5 - D			
103	2440	2740	3.4	3.3	91.0
104	2440	2740	3.4	3.4	91.2
105	2740	3010	4.2	4.1	92.2
106	2740	3050	4.1	4.1	92.8
107	2970	3260	4.9	4.8	93.0
108	2970	3320	5.2	5.1	93.6
109	3250	3610	6.2	6.0	94.6
110	3250	3580	6.2	6.1	94.2

INVESTIGATIONS OF A CYCLONE
DUST COLLECTOR

by

WILLIAM WOODROW DODGE

B. S., Oklahoma A. and M. College, 1941

M. S., Kansas State College
of Agriculture and Applied Science, 1949

AN ABSTRACT OF A THESIS

submitted in partial fulfillment of the

requirements for the degree

MASTER OF SCIENCE

Department of Applied Mechanics

KANSAS STATE COLLEGE
OF AGRICULTURE AND APPLIED SCIENCE

1951

The cyclone dust collectors used in this research were built in sections so that the parts could be interchanged to give dust collectors of differing dimensions. The inlet was varied in shape but had a constant cross sectional area of 16 square inches. Four different cone sections of 1, 2, 3 and 4 diameters in length were used. There were three outlet tubes with cross sectional areas of 10.67, 16 and 24 square inches. These outlet tubes were made so as to slide freely in the covers to facilitate varying the length to which the outlet tube extended into the collector.

It was found that as the cone length was increased the efficiency of dust collection increased. The 4 diameter cone was the most efficient used in this experiment. Indications were found that a cone longer than 4 diameters might in some cases have even greater efficiency.

With other factors held constant it was found that the 4 inch high cylindrical section was the most efficient in percentage dust collection with the 8 inch section, the 16 inch section, and the 12 inch section following in order of decreasing efficiency. It was found that as the outlet area was increased the collection efficiency decreased somewhat but that the pressure drop decreased very appreciably. As the inlet velocity was increased the collection efficiency increased as did the pressure drop across the collector. The extent to which the outlet tube extended down into the

collector affected the efficiency very considerably. Three positions were investigated, first, the outlet tube did not extend into the collector; second, the outlet tube extended down half of the height of the cylindrical section; and third, the outlet tube extended down to the top of the cone. The first was found to be less efficient than the other two, the half position being slightly better than the down position.

A complete map of the tangential velocities inside the collector was made with the aid of a Prandtl pitot tube. The tangential component of velocity was found to be almost identical with that of the Rankine combined vortex. The departure was thought to be due to friction and turbulence. Measurements of the radial and axial components of velocity were not taken.